Neurotherapeutics 21 (2024) e00388

Contents lists available at ScienceDirect

Neurotherapeutics

journal homepage: www.sciencedirect.com/journal/neurotherapeutics

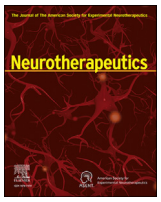

Original Article

Reversal of cognitive deficits in FUS^{R521G} amyotrophic lateral sclerosis mice by arimoclomol and a class I histone deacetylase inhibitor independent of heat shock protein induction

Mari Carmen Pelaez [a], Frédéric Fiore [b,1,3], Nancy Larochelle [c,3], Afrooz Dabbaghizadeh [c,2,3], Mario Fernández Comaduran [c], Danielle Arbour [b], Sandra Minotti [c], Laetitia Marcadet [a], Martine Semaan [b], Richard Robitaille [b], Josephine N. Nalbantoglu [c], Chantelle F. Sephton [a,4], Heather D. Durham [c,4,*]

[a] *Department of Psychiatry and Neuroscience, CERVO Brain Research Centre, Laval University, Quebec City, QC Canada*
[b] *Département de Neurosciences and Groupe de Recherche sur le Système Nerveux Central, Université de Montréal, and Centre Interdisciplinaire de Recherche sur le Cerveau et l'apprentissage, Montréal, QC Canada*
[c] *Department of Neurology & Neurosurgery and Montreal Neurological Institute, McGill University, Montreal, QC Canada*

A R T I C L E I N F O

Keywords:
Amyotrophic lateral sclerosis
Heat shock proteins
FUS
Arimoclomol
Histone deacetylase inhibitor
Frontotemporal dementia

A B S T R A C T

Protein misfolding and mislocalization are common to both familial and sporadic forms of amyotrophic lateral sclerosis (ALS). Maintaining proteostasis through induction of heat shock proteins (HSP) to increase chaperoning capacity is a rational therapeutic strategy in the treatment of ALS. However, the threshold for upregulating stress-inducible HSPs remains high in neurons, presenting a therapeutic obstacle. This study used mouse models expressing the ALS variants FUS^{R521G} or SOD1^{G93A} to follow up on previous work in cultured motor neurons showing varied effects of the HSP co-inducer, arimoclomol, and class I histone deacetylase (HDAC) inhibitors on HSP expression depending on the ALS variant being expressed. As in cultured neurons, neither expression of the transgene nor drug treatments induced expression of HSPs in cortex, spinal cord or muscle of FUS^{R521G} mice, indicating suppression of the heat shock response. Nonetheless, arimoclomol, and RGFP963, restored performance on cognitive tests and improved cortical dendritic spine densities. In SOD1^{G93A} mice, multiple HSPs were upregulated in hindlimb skeletal muscle, but not in lumbar spinal cord with the exception of HSPB1 associated with astrocytosis. Drug treatments improved contractile force but reduced the increase in HSPs in muscle rather than facilitating their expression. The data point to mechanisms other than amplification of the heat shock response underlying recovery of cognitive function in ALS-FUS mice by arimoclomol and class I HDAC inhibition and suggest potential benefits in counteracting cognitive impairment in ALS, frontotemporal dementia and related disorders.

* Corresponding author.
E-mail addresses: maria-del-carmen.pelaez-brenes.1@ulaval.ca (M.C. Pelaez), frederic.fiore@uni-heidelberg.de (F. Fiore), nancy.larochelle@mcgill.ca (N. Larochelle), Afrooz.dabbaghi@gmail.com (A. Dabbaghizadeh), mario.fernandez@mcgill.ca (M.F. Comaduran), danielle.arbour@umontreal.ca (D. Arbour), sandra.minotti@mcgill.ca (S. Minotti), laetitia.marcadet.1@ulaval.ca (L. Marcadet), martine.semaan@umontreal.ca (M. Semaan), richard.robitaille@umontreal.ca (R. Robitaille), josephine.nalbantoglu@mcgill.ca (J.N. Nalbantoglu), chantelle.sephton.1@ulaval.ca (C.F. Sephton), heather.durham@mcgill.ca (H.D. Durham).
[1] Fiore present address: The Chica and Heinz Schaller Research Group, Institute for Anatomy and Cell Biology, Heidelberg University, Heidelberg, Germany.
[2] Dabbaghizadeh present address: Centre de Recherche du Centre hospitalier de l'Université de Montréal (CRCHUM), Montréal, QC Canada.
[3] Equal contribution.
[4] Shared senior authorship.

https://doi.org/10.1016/j.neurot.2024.e00388
Received 8 April 2024; Received in revised form 14 June 2024; Accepted 15 June 2024

Introduction

Protein misfolding and aggregation are common themes in neurodegenerative diseases, including both familial and sporadic forms of amyotrophic lateral sclerosis (ALS). They can occur as a direct consequence of genetic mutations, from posttranslational modifications, or from a general compromise in proteostasis. A key mechanism regulating protein quality control is the chaperoning activity of heat shock proteins (HSPs), which work collaboratively to sequester misfolded proteins to prevent inappropriate interactions, to restore proper folding, or to target them for degradation. Upregulating HSP expression has been pursued as a logical therapeutic strategy in disorders like ALS, but applying HSP-based therapy in patients has proven challenging.

In general, environmental and physiological stresses that increase the load of misfolded proteins activate transcription of *HSP* genes, a process known as the heat shock response. The major transcription factor is heat shock transcription factor 1 (HSF1), which binds to heat shock elements (HSE) on *HSP* gene promoters. HSF1 is sequestered in a multichaperone complex including HSP90 and HSP70. Upon stress, misfolded proteins compete for these HSPs, releasing HSF1, which then bind as trimers to HSE [1,2]. Indeed, inhibitors that disrupt these HSP90 complexes upregulate HSPs, including the stress-inducible isoform HSPA1A [3]. Although HSP90 inhibitors have been neuroprotective in preclinical models of neurodegeneration including ALS [4,5], they tend to have a low therapeutic window due to toxicity, and sensitivity can be lost over time, as in the case of the R6/2 mouse model of Huntington's disease treated with the inhibitor HSP990 [6].

Arimoclomol is a hydroxylamine that enhances an existing heat shock response by promoting HSF1 binding to HSE, *i.e.,* acting as an HSP co-inducer [7]. The attractiveness of this class of agents is that HSPs would be produced according to demand with less potential for toxicity compared to constitutive upregulation. Arimoclomol showed promise in preclinical models [8,9], but a phase III clinical trial in sporadic ALS failed to meet primary endpoints [10].

HSF1 binding to HSE is not sufficient to initiate transcription, subsequent steps being required to activate HSF1 [2]. Many classes of neurons including spinal motor neurons *in vivo* [11] and in culture [12] have a high threshold for activating HSF1 and mounting a heat shock response to thermal stress or to proteotoxic stress such as expression of genetic variants linked to familial ALS. This property could contribute to the vulnerability of motor neurons in ALS by allowing the accumulation of toxic misfolded proteins and putting stress on proteolytic mechanisms. The same property likely contributes to the failure of drugs like arimoclomol designed to magnify the heat shock response. Efficacy would depend not only on some activation of the pathway by the stress, but on transactivational competence, both of which appear to be compromised in neurons.

Regulation of HSF1 is complex, but epigenetic mechanisms including histone acetylation certainly play a major role in *HSP* expression normally and in ALS. The chromatin landscape dictates the stress-inducible binding of HSF1 to HSE. Binding occurs at areas of open chromatin with tetra-acetylated H4 and acetylated H3K9 marks [13]. The desensitization of R6/2 mice to HSP990 was attributed to reduction in H4 tetra-acetylation as part of the disease process [6]. The reduction in acetylation of H3K9/14 in motor neurons expressing ALS-linked FUS or TDP-43 variants could have a comparable effect [14]. We previously reported that inhibitors of class I histone deacetylases (HDAC) and the pan HDAC inhibitor, suberoylanilide hydroxamic acid (SAHA) acted as HSP co-inducers comparable to arimoclomol, in cultured motor neurons with proteotoxic stress induced by the ALS-linked variant $SOD1^{G93A}$, and could enhance expression of HSPA1A when combined with either arimoclomol or with an HSP90 inhibitor that constitutively induced HSPs [15]. However, the response to proteotoxicity and to drug treatments varied with the form of familial ALS being modeled; *e.g.,* no HSPA1A or increase in the constitutively expressed heat shock cognate protein HSPA8 was detected in neurons expressing the FUS^{R521G} variant with or without drug treatment, indicating shut down of the heat shock response [15,16]. Nevertheless, treatments were neuroprotective independent of HSP induction, including preservation of FUS and the nBAF chromatin remodeling complex component Brg1 in the nucleus [15,16].

The next step was to extend this knowledge derived in culture models to the *in vivo* context using mouse models of familial ALS caused by mutations in *SOD1* and *FUS*, specifically $SOD1^{G93A}$ transgenic mice (a.k.a. Gurney mice from The Jackson Laboratory) [17] and mice globally expressing the human FUS variant p.R521G, $hFUS^{R521G/Meox2}$ (FUS^{R521G} mice) produced by the Sephton lab (see Methods). We have determined the effect of the transgenes and of treatments with a CNS-permeant inhibitor of class I HDACs, RGFP963, arimoclomol and the drug combination on expression of a panel of HSPs in CNS and muscle tissue, in comparison to performance on behavioral tests and neuromuscular function. Effects on HSP expression were qualitatively similar to findings in the culture models. Of particular importance, we report that in the ALS-FUS mice, arimoclomol, and RGFP963, actually restored performance on cognitive tests, despite no change in expression of HSPs. The data point to alternative neuroprotective mechanisms exerted by these drugs and potential benefit in disorders with cognitive impairment.

Materials and Methods

Mouse models of familial ALS

FUS ALS: $hFUS^{R521G/Meox2Cre}$ (FUS^{R521G}) mice were produced by crossing *CAG-Z-FUSR521G-IRES-EGFP* mice with Meox2Cre mice (Control) [18] to induce global expression of the human FUS^{R521G} variant. Genotypes of all animals were determined by PCR, using the following primers: *FUS* (forward: 5' GAC CAG GTG GCT CTC ACA TG 3'; reverse: 5' GTC GCT ACA GAC GTT GTT TGT C 3') and Cre (forward: 5' GGA CAT GTT CAG GGA TCG CCA GGC 3'; reverse: 5' GCA TAA CCA GTG AAA CAG CAT TGC 3'). Note this mouse line expresses total FUS at similar levels to wild type mice [18].

SOD1 ALS: Male transgenic mice overexpressing the human $SOD1^{G93A}$ transgene [17] (stock #002726) and B6 (non-carrier littermates, control) were obtained from The Jackson Laboratory (JAX). Genotyping was carried out by JAX and human SOD1 expression was verified by Western analysis.

Drug treatment

Mice were injected *i.p.* with the class I HDAC inhibitor, RGFP963 (BioMarin Pharmaceutical Inc.), arimoclomol (Medkoo Biosciences) or the combination at indicated dosages in a solution containing 45% normal saline, 50% polyethylene glycol 300 (Sigma-Aldrich) plus 4.8% dimethyl sulfoxide (DMSO) or vehicle alone. Dosage for arimoclomol was obtained from the literature [8,19]. Dosage of RGFP963 was inferred from pharmacokinetic data provided by the supplier and target engagement in mouse CNS was determined by inhibition of class I HDACs in homogenates of cortex as described in Fig. S1.

FUS^{R521G} mice were treated for 28 days (7 days/week) starting at P60, when behavioral deficits are present (*vide infra*). $SOD1^{G93A}$ mice were treated 5 days/week from P50-P75 (for evaluation of neuromuscular parameters), P75-105 (beginning prior to motor neuron loss) or during the symptomatic phase from P105 to endstage (onset of hindlimb paralysis) [17].

Behavioral testing of FUS mice

Behavioral tests were conducted as previously described [20] and summarized below. Testing was performed 7 days before treatment and 7 days after treatment. The total number of mice (male (M) and female (F)) tested for each experimental condition included 32 (16M:16F) littermate controls - vehicle (+/+; +/+, +/+; +/Cre, Tg/+; +/+); FUS^{R521G} (Tg/+; +/Cre) mice: 34 (19M:15F) - vehicle, 13 (6M:7F) −10 mg/kg

RGFP963, 12 (8M:4F) - 20 mg/kg RGFP963, 9 (6M:3F) - 5 mg/kg arimoclomol, 10 (5M:5F) - 10 mg/kg arimoclomol, 9 (5M:4F) - 20 mg/kg arimoclomol, 7 (2M:5F) – 5 mg/kg arimoclomol combo, and 11 (5M:6F) – 20 mg/kg arimoclomol combo.

Novel object recognition test to assess memory

On the first day of the test, mice were introduced to the arena and allowed to explore for 5 min. On the second day, two identical objects (familiar objects) were presented to the mice for a maximum of 5 min. On the third day, 24 h after the presentation of the familiar objects, animals were exposed to one familiar and one novel object for 5 min. Interaction time with each object during the duration of the test was recorded.

Passive avoidance test to assess memory in a fear-aggravated environment

The apparatus consists of equal-sized light and dark compartments separated by a door and an electrified grid. On the first day, mice were placed in the light chamber; after 30 s the door was opened allowing the animals to cross to the dark chamber and get familiarized with the arena. On the second day, mice were introduced into the light chamber; after 30 s the door was opened and mice were allowed to cross to the dark chamber, where immediately after entry, an electrical foot shock (0.5 mA for 2 s) was delivered. Twenty-four hours after the foot-shock, mice were re-introduced to the light chamber. The door was opened after 5 s, and the latency time to cross from the light to the dark chamber was measured to a maximum of 5 min.

Rotarod test of motor function

Mice were placed on a stationary rotarod, which was accelerated at 0.1 rpm/s for a total of 5 min. The latency time to fall from the rod was recorded for each mouse. Each mouse was tested four times a day for 2 consecutive days with an inter-trial interval of at least 10 min.

Hanging wire test

Mice were placed on a horizontal wire 50 cm above a layer of soft bedding, flipped upside down and latency to fall was measured up to a maximum of 300 s.

Grip strength

All-limbs grip strength was measured using a machine from *BioSeb* and a custom-made metal grid. The animals were placed on all four limbs in the center of the grid, then firmly pulled off the grid by the tail. Each session consisted of 3 rounds (3 pulls per round), with the round with greatest force being kept. The final output for each session corresponds to the average force generated from those 3 rounds. Muscle strength were assessed using the BIO-GS3 grip strength meter (Bioseb, France). Mice were placed on a wire grid and gently pulled backward by the tail. Absolute grip strength was measured in grams and normalized to body weight.

Immunocytochemistry and image analysis of FUS mice

FUS mice were anesthetized with ketamine/xylazine (100/10 mg/kg) and perfused with 0.9% saline and 4% paraformaldehyde (PFA). Cortex and spinal cord samples were post-fixed for 24 h in 4% PFA, and cryoprotected in 30% sucrose solution for 24–48 h at 4°C. 40 µm microtome sections (Microm HM430, ThermoFisher) were washed 3 × 10 min with PBS, followed by 1 h blocking with 3% BSA, 5% FBS, 0.3% Triton 100X and 0.02% sodium azide in PBS. Sections were incubated overnight at 4°C with primary antibodies diluted in 1% BSA, 3% fetal bovine serum (FBS), 0.3% Triton 100X, and 0.02% sodium azide in PBS. The next day, sections were washed 3 times with PBS followed by incubation with Alexa Fluro-conjugated secondary antibodies diluted in incubation solution for 2 h at room temperature in the dark. Sections were washed 3 times with PBS and mounted onto glass slides using VECTASHIELD Antifade Mounting Medium with DAPI (Vector Laboratories, VECTH1200). Imaging was performed using a Zeiss LSM710 inverted confocal and imaged as z-stacks (1–2 µm steps per stack) from 3 to 4 biological replicates per group. Maximum intensity projection images for 5–7 images per biological replicate were analyzed using Fiji ImageJ signal intensity measuring tool.

Synaptophysin (SYP) and PSD-95 imaging was performed using a Nikon A1 confocal microscope, 63× oil immersion objective, collecting z-stacks images (1 µm steps per stack) from 3 to 5 nonoverlapping images of 3 biological replicates per group. Puncta were counted using the spot-detection function of IMARIS (software version 10.0, Oxford Instruments, UK). For colocalization, spot-detection was combined with shortest distance to spots-spots filter.

Primary antibodies were: rabbit anti-FUS (Sigma HPA008784, 1:500), FluoTag®-X2 AZDye568 anti-PSD-95 (NanoTag Biotechnologies N3702-AF568L, 1:500), mouse anti-SYP (Synaptic Systems 101011, 1:250).

Secondary antibodies were from Invitrogen and used at 1:500: Alexa Fluor 488 goat anti-mouse IgG (A11001), Alexa Fluor 488 goat anti-rabbit IgG (A11034), Alexa Fluor 546 goat anti-mouse IgG (A11030), Alexa Fluor 546 goat anti-rabbit IgG (A11035), Alexa Flour 647 goat anti-mouse IgG (A211236) and Alexa Flour 647 goat anti-rabbit IgG (A211245).

Golgi staining and Sholl analysis of FUS mice

Golgi staining was carried out according to manufacturer's instructions as previously described [21] using FD Rapid GolgiStain™ kit (FD Neurotechnologies Inc.) on cortical and spinal cord cryostat sections (Cryostat NX50, Thermo Scientific) mounted on gelatin-coated slides (1% gelatin and 0.1% chromium potassium sulphate dodecahydrate).

Cortical and spinal motor neuron images were taken using a Zeiss AxioImager.M2 microscope and a 40× oil immersion lens and 20× objectives. Cortical neurons from layers IV-V of the M1 and M2 brain regions and spinal motor neurons located at the ventral horn of the spinal cord were selected for the analysis. Motor neurons were 3D-reconstructed using Neurolucida 360 software (MBF Bioscience) as previously described [20]. Spine detection was performed in Neurolucida 360 of the apical dendrite of cortical motor neurons at a 30–100 µm distance from the soma. Spines were classified according to their shape: mushroom-shaped spines were considered “mature” whereas thin filopodia or stubby-shaped spines were considered “immature”, and spine density was calculated. Sholl and spine analysis was performed on 10 individual neurons from 3 biological replicates per group for a total of 30 neurons.

Immunohistochemistry and image analysis of SOD1 mice

For immunohistochemistry, tissues were collected in 50 ml tubes containing 10% Buffered Formalin (Fisher Scientific, 23245684) following euthanasia and perfusion of mice with normal saline. After 48 h, tissues were transferred to 70% ethanol and transported to the MUHC Research Institute Histology Platform for processing, paraffin embedding, and cutting and mounting of serial cross-sections (4 µM thickness, 2 sections per slide). Sections were deparaffinized in xylene, rehydrated in ethanol and rinsed with distilled water. For antigen retrieval, sections were boiled in 10 mM sodium citrate +0.05% Tween pH6.0 for 10 min, cooled for 20–30 min and rinsed in TBS, followed by blocking in 10% horse serum (HS) + 3% BSA + 0.3% Triton-X100 in TBS for 1.5–2 h. Antibodies were diluted in 10% HS in TBS. Sections were outlined using a delimiting Pen (Dako S2002) to restrict antibody distribution. Primary antibodies were applied overnight at 5 °C in a humidified chamber. Endogenous peroxidase was quenched in 0.6% hydrogen peroxide for 10 min. Secondary antibodies were biotinylated anti-mouse IgG (H+L), anti-rabbit IgG (H+L) or anti-goat IgG (H+L) (Vector Laboratories) or peroxidase-conjugated anti-rabbit IgG (Jackson ImmunoResearch), applied at 1:500 at room temperature for 1 h. For biotinylated secondary antibodies, VECTASTAIN Elite ABC-HRP Kit (Vector Laboratories, PK-

6100) was employed for 1 h. All steps were followed by 3 × 2 min rinses in TBS. ImmPACT DAB HRP Substrate (Vector Laboratories, SK4105) was applied for 5–10 min prior to mounting in Immu-Mount (Epredia, 9990412). Primary antibodies were: mouse anti-HSPA1A (StressMarq smc-100, 1:100), rabbit anti-HSPA8 (StressMarq smc-151, 1:100), goat anti-HSPB1 (Santa Cruz sc-1049, 1:100), mouse anti-hypophosphorylated neurofilament SM132 (Biolegend 801701, 1:1000) and rabbit anti-glial fibrillary acidic protein (GFAP) (Dako Z0334, 1:400).

Western analysis

Mice were euthanized by deep anesthesia with isoflurane (SOD1 mice) or ketamine/xylazine (FUS mice) and perfused with normal saline. Cortex, lumbar spinal cord, and skeletal muscle (gastrocnemius/soleus) were harvested and stored at −80 °C. Immediately after thawing, tissue samples were homogenized in buffer containing 50 mM Tris-HCl pH 7.4 and 10% glycerol using Bullet Blender (Next Advance) and aliquots were kept at −80 °C.

Tissue homogenates were diluted in lysis buffer (50 mM Tris-HCl pH 7.4, 2% SDS 10% glycerol) supplemented with protease inhibitor cocktail (Sigma Aldrich) and 5 mM sodium butyrate (Bio Basic Inc.). Homogenates were sonicated for 5–10 s at 50 % cycle using an Ultrasonic homogenizer 4710 series (Cole Parmer Instrument Co., Chicago, IL USA) and protein concentrations were determined using the DC protein assay (Bio-Rad Laboratories). Twenty-five μg of protein were separated by 10–15% SDS-PAGE. After transfer to nitrocellulose, membranes were blocked in 5% skim milk in TRIS-buffered saline (TBS) plus 0.05% Tween 20 (TBST) and probed with primary antibodies, then HRP-conjugated secondary antibodies in 5% skim milk. Labeling was detected using ECL Prime Detection Reagent (Amersham, RPN2236). Images were acquired with an Intas Imaging System (Intas GmbH) and densitometry of bands was performed using NIH ImageJ software. Bands of interest were normalized to loading controls (as indicated in the figures), followed by normalization to the vehicle-treated control.

Primary antibodies were: mouse anti-HSPA1A (StressMarq smc-100, 1:500), mouse anti-HSPA8 (StressMarq smc-151, 1:1000), rabbit anti-HSP70 (Enzo ADI-SPA812, 1:1000), goat anti-HSPB1 (Santa Cruz sc-1049, 1:1000), rabbit anti-HSP40 (Enzo ADI-SPA-400, 1:2000), mouse anti-HSP90 (StressMarq smc-149, 1:000), rabbit anti-α-tubulin (Abcam 15246, 1:10,000), mouse anti-tubulin acetylated (Sigma T6793, 1:10,000), mouse anti-STIP1(Abnova H00010963-M11, 1:1000), rat anti-HSF1 (StressMarq smc-118, 1:1000), rabbit anti-HDAC3 (Sigma H3034, 1:1000), mouse anti-α-tubulin (MediMabs MM-0163, 1:20,000), mouse anti-actin (Mp Biochemicals 691002, 1:20,000), mouse anti-GAPDH (MediMabs MM-0163, 1:5000), rabbit anti-SOD1 (Enzo ADI-SOD-101, 1:5000), rabbit anti-FUS ((Proteintech 11570-1-AP, 1:1000) and mouse anti-FUS (Santa Cruz, sc-47711, 1:1000). Peroxidase-conjugated secondary antibodies were from Jackson ImmunoResearch: goat anti-mouse (115-035-044, 1:5000), donkey anti-rabbit (711-035-152, 1:5000), rabbit anti-goat (305-035-045, 1:5000) and goat anti-rat (112-035-167, 1:5000).

Evaluation of neuromuscular junction and muscular properties of SOD1 mice

At P75, mice were euthanized and Extensor Digitorum Longus (EDL) nerve-muscle preparations were isolated in oxygenated normal Rees' Ringer solution: (in mM) 110 NaCl, 5 KCl, 1 $MgCl_2$, 25 $NaHCO_3$, 2 $CaCl_2$, 11 glucose, 0.3 glutamate, 0.4 glutamine, 5 BES, 4.34 x 10^{-7} cocarboxylase and 3.6 x 10^{-5} choline chloride. A C-1 curved needle and 6-0 suture wire (Ethicon) were then used to tie knots on both tendons of the muscle before installing it vertically on the force transducer (Aurora Scientific) (Fig. S11D). Once mounted, the muscle was stretched to the length at which stimulation generated the largest force and the nerve was suctioned into a Ringer-filled pipette for stimulation. A stimulation electrode and a reference electrode were placed near the muscle in the bath of oxygenated Ringer solution.

Muscle contraction was evoked by stimulating the nerve (1 V) or the muscle directly (50 V) using a Grass S88 stimulator (Grass Instruments) coupled to an IsoFlex (A.M.P.I., Israel). The resulting contractile force was converted to an electrical signal by the force transducer, which was then passed through a 2 kHz low-pass filter (DC amplifier/filter, Warner Instruments) and digitalized (BNC-2110, National Instruments). The signal was acquired and analyzed using WinWCP 5.3.2 (John Dempster, Strathclyde University, United Kingdom).

Force/frequency curve

Each EDL underwent the same two stimulation protocols. First, both the nerve and the muscle were stimulated sequentially, at 2-min intervals, at frequencies ranging from 5 to 300 Hz (Fig. S11). Each nerve stimulation was followed by muscle stimulation (and vice-versa), until all 18 frequencies had been recorded for both nerve and direct muscle stimulation. Baseline force was constantly monitored to ensure that the tension in the muscle was ideal throughout.

Fatigue and recovery

A 120 Hz stimulus was applied every second (9 times to the nerve, once to both the nerve and the muscle; repeated 18 times) for 180 s. Recovery was then assessed by measuring the contraction force sporadically over the following 30 min. After each experiment, the preparations were fixed in 4% formaldehyde for 10 min, washed 3 x for 5 min in PBS and kept at 4 °C until further processing.

Neuromuscular junction immunofluorescence

Muscles were permeabilized in 100% methanol at −20 °C for 6 min, washed 3 × 5 min in PBS, and then immersed in a PBS solution containing 0.01% Triton X-100 and 10% normal donkey serum (NDS) for 20 min at room temperature. The muscles were sequentially incubated with primary antibodies against S100 (Rabbit anti-S100 IgG, Dako IR-504, 1:4), neurofilament M (NFM) (Chicken anti-NFM IgY, Rockland, 1:1000) and SV2 (Mouse anti-SV2 IgG1, DSHB, 1:2000) in 1% Triton X-100 and 2-10% normal donkey serum in PBS for 2 h at room temperature. After washing PBS 3-4 x 5 min, the muscles were incubated with secondary antibodies from Jackson ImmunoResearch (Alexa 647-conjugated donkey anti-rabbit IgG (1:500), Alexa 488-conjugated donkey anti-chicken IgG (1:500), Alexa 448-conjugated donkey anti-mouse IgG1 (1:500), as well as with Alexa 594-conjugated α-bungarotoxin (Invitrogen, 1:500) for 1–1.5 h at room temperature. Finally, the muscles were placed on microscope slides, immersed in ProLong Gold Antifade (Invitrogen) and sealed with nail polish. Z-stack images were acquired using the Olympus FV-1000 confocal microscope and analyzed using the Fluoview software.

Results

Treatment with RGFP963, arimoclomol or the combination improved cognitive performance of FUS^{R521G} mice

The germline FUS^{R521G} mice develop social and motor deficits and neuroinflammation [18]. By 2 months of age, they showed significant impairment in passive avoidance and novel object recognition tests, which measure memory and cognitive function [20], in comparison to littermate control mice (Figs. S2A and B). At this age, FUS^{R521G} mice also have modest motor impairment measured by latency to fall from the rotarod (Fig. S2C). Mice were retested following 4 weeks of treatment with arimoclomol, the class I histone deacetylase (HDAC) inhibitor RGFP963, or drug combination by daily *i.p.* injection. Both RGFP963 and arimoclomol produced dose-dependent improvement in cognitive behavior (Fig. 1A and B).

Compared to vehicle-treatment, FUS^{R521G} mice treated with 20 mg/kg RGFP963 showed improvement in passive avoidance (Fig. 1A) and

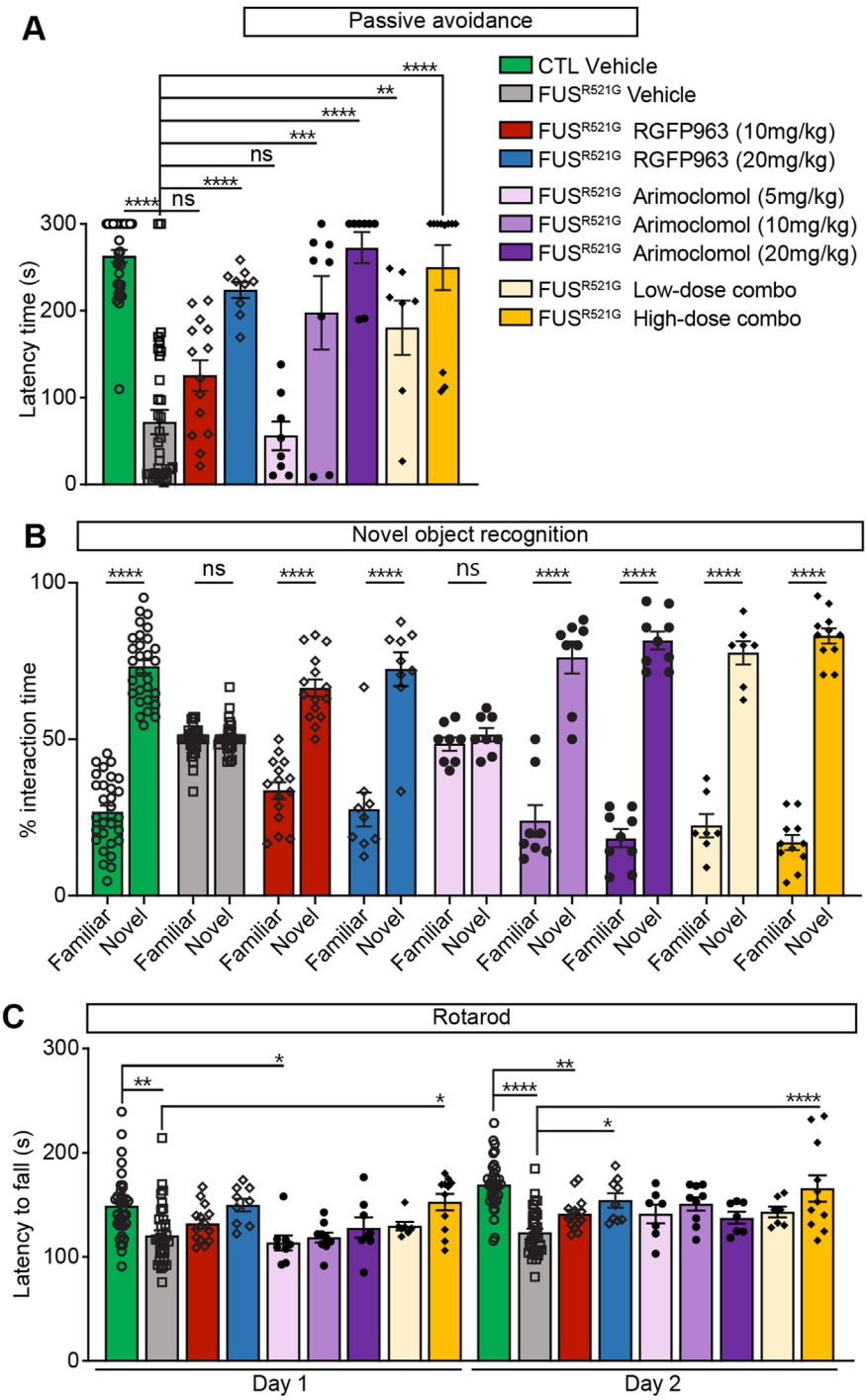

Fig. 1. Treatment with RGFP963, arimoclomol or drug combinations improved cognitive performance in FUS^{R521G} mice. (A) Passive avoidance test: $hFUS^{R521G/Meox2Cre}$ (FUS^{R521G}) mice treated with 20 mg/kg RGFP963, 10 or 20 mg/kg arimoclomol, or the low-dose (5 mg/kg arimoclomol + 10 mg/kg RGFP963) and high-dose (20 mg/kg arimoclomol + 10 mg/kg RGFP963) combinations showed a significant increase in latency time in entering the dark compartment after aversive shock preconditioning compared to vehicle-treated FUS^{R521G} mice. (B) Novel object recognition test: CTL and FUS^{R521G} mice treated with 10 or 20 mg/kg RGFP963, 10 or 20 mg/kg arimoclomol, or the low- or high-dose combinations spent more time interacting with the novel object versus the familiar object, whereas vehicle-treated FUS^{R521G} mice spend equal time interacting with both objects. (C) Rotarod test: FUS^{R521G} mice treated with RGFP963 or the high-dose combination stayed longer on the rotarod. Values from each group are expressed as mean ± SEM. Statistical analysis was by unpaired Student's *t*-test for comparisons between two groups and a one-way ANOVA with Bonferroni correction test for comparisons between more than 2 groups. mice/group: CTL mice - vehicle (32); FUS^{R521G} mice - vehicle (34), 10 mg/kg RGFP963 (13), 20 mg/kg RGFP963 (12), 5 mg/kg arimoclomol (9), 10 mg/kg arimoclomol (10), 20 mg/kg arimoclomol (9), low-dose combo (7), high-dose combo (11)). $^{*}p < 0.05$, $^{**}p < 0.01$, $^{***}p < 0.005$, $^{****}p < 0.001$, and not significant (ns).

novel object recognition (Fig. 1B), whereas mice treated with 10 mg/kg showed only improvement in the novel object recognition test. Mice treated with 20 mg/kg arimoclomol showed full reversal of deficits in both the passive avoidance and novel object recognition tests, performing equivalent to vehicle-treated littermate controls. The dose of 10 mg/kg arimoclomol had a reversal effect on both tests, but 5 mg/kg arimoclomol had no effect. In the passive avoidance test, the low-dose combination of 5 mg/kg arimoclomol with 10 mg/kg RGFP963 (both showing no effect individually) improved performance, indicating a synergistic effect (Fig. 1A). In the novel object recognition test, all treatment groups except 5 mg/kg arimoclomol, the no effect level, showed an increase in the percentage of interaction time with a novel object (Fig. 1B).

Improved motor function occurred in mice treated with 20 mg/kg RGFP963 and the high-dose combination, but not with arimoclomol alone or the other treatment regimens (Fig. 1C). Thus, treatment with arimoclomol and RGFP963 reversed profound cognitive deficits in mice expressing the ALS-associated FUS^{R521G} variant with minimal effect on motor function.

Combined treatment with arimoclomol and RGFP963 improved motor neuron dendritic branching and cortical motor neuron synaptic densities

The expression of ALS-FUS variants in multiple models reduces neuronal arborization and structural complexity as well as synaptic connectivity and integrity [18,20–24]. The data showing impairment in

cortical and motor neuron dendritic arbors of FUS^{R521G} mice compared to wild-type mice was previously reported [18,20]. For the present study, we focused on comparing morphology of cortical and spinal motor neurons of FUS^{R521G} mice treated with vehicle compared to those administered 20 mg/kg arimoclomol, 10 mg/kg RGFP963 or the combination. The combination, but not the drugs individually, improved dendritic structures, as indicated by an increase in the number of dendritic intersections and thickness of dendritic branches (Fig. 2). These drug treatments had similar effects on spinal motor neuron dendritic branching and cumulative area (Fig. 3A and D).

The 20 mg/kg arimoclomol combination with RGFP963 (high-dose combination) as well as RGFP963 or arimoclomol individually did increase the number of mature spines and density of mature dendritic spines on cortical motor neurons in FUS^{R521G} mice (Fig. 4A–C). The increased number of mature post-synapses in mice treated with the high-dose combination corresponded to an increase in synaptic densities as determined by the co-localization of both pre-synaptic and post-synaptic markers, indicating that this treatment promotes synaptic connectivity within the cortex (Fig. 4D–G). Collectively, the analysis of neuronal arborization and synapses show that individual treatment with RGFP963 or arimoclomol is sufficient to improve the spine density of cortical motor neurons; however, a synergistic effect of these two drugs is required to improve dendritic branching.

We then assessed the neuromuscular junctions (NMJs) from the extensor digitorum longus (EDL) of FUS^{R521G} mice (Fig. S3) and found no significant change in the innervation profile between littermate controls and FUS^{R521G} mice. EDL innervation was not compromised significantly in the FUS^{R521G} mice, thus not accounting for the modest reduction in Rotarod performance. Moreover, there was no significant effect of either individual treatment and the high-dose combination treatment was potentially damaging (Fig. S3).

Neither expression of FUS^{R521G} nor drug treatments altered expression of HSPs in cortex or skeletal muscle

The original premise of this study was to facilitate upregulation of HSPs with chaperoning activity to improve neuroprotection in ALS models. As in the culture model of FUS ALS, both RGFP963 and arimoclomol demonstrated neuroprotective properties *in vivo* in FUS^{R521G} mice. In cultured motor neurons, the heat shock response was impaired by FUS variants and did not account for efficacy of the drug treatments [15,16]. We measured levels of a variety of HSPs in homogenates of cortex and skeletal muscle of FUS^{R521G} mice by Western analysis; *i.e.*, the inducible HSP70 isoform, HSPA1A, and the constitutively expressed HSPA8; HSP40, a DNAJ protein acting with HSP70 in ATP-dependent protein refolding; HSP90 important for transcription factor regulation

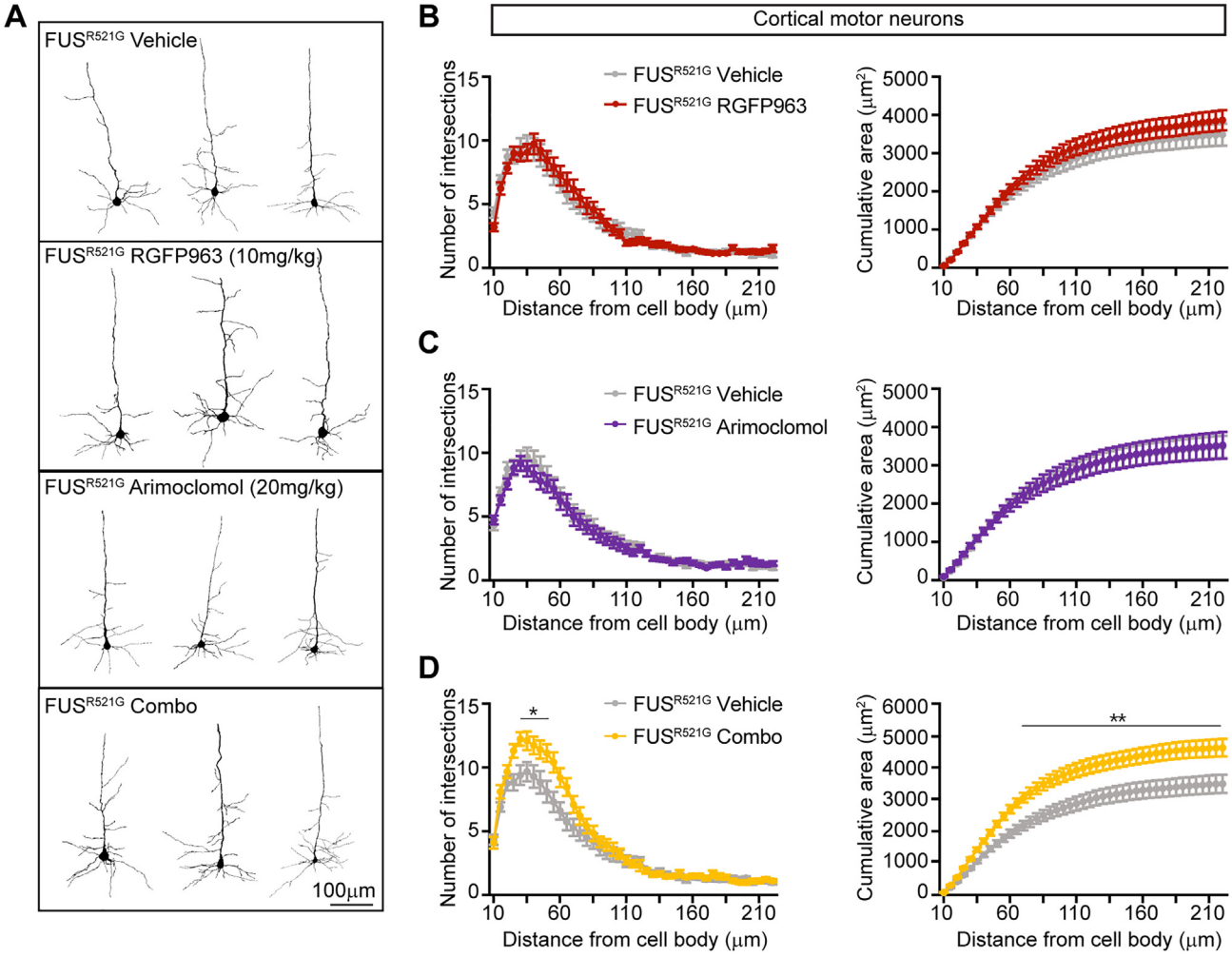

Fig. 2. Combined treatment with arimoclomol and RGFP963 promoted cortical motor neuron dendritic branching. (A) Neurolucida tracing of cortical motor neurons from FUS^{R521G} mice treated with vehicle, 10 mg/kg RGFP963, 20 mg/kg arimoclomol or the combination. Sholl analysis showing no significant changes in dendritic intersections and cumulative area of dendrites in (B) RGFP963- or (C) arimoclomol-treated mice, but a significant increase in dendritic branching and cumulative area in mice treated with (D) the combination. Values from each group are expressed as mean ± SEM. Statistical analysis was determined with a two-way repeat measures ANOVA with Bonferroni correction test for Sholl analysis (n = 3 mice/group). *$p < 0.05$, **$p < 0.01$, ***$p < 0.005$ ****$p < 0.001$, and not significant (ns).

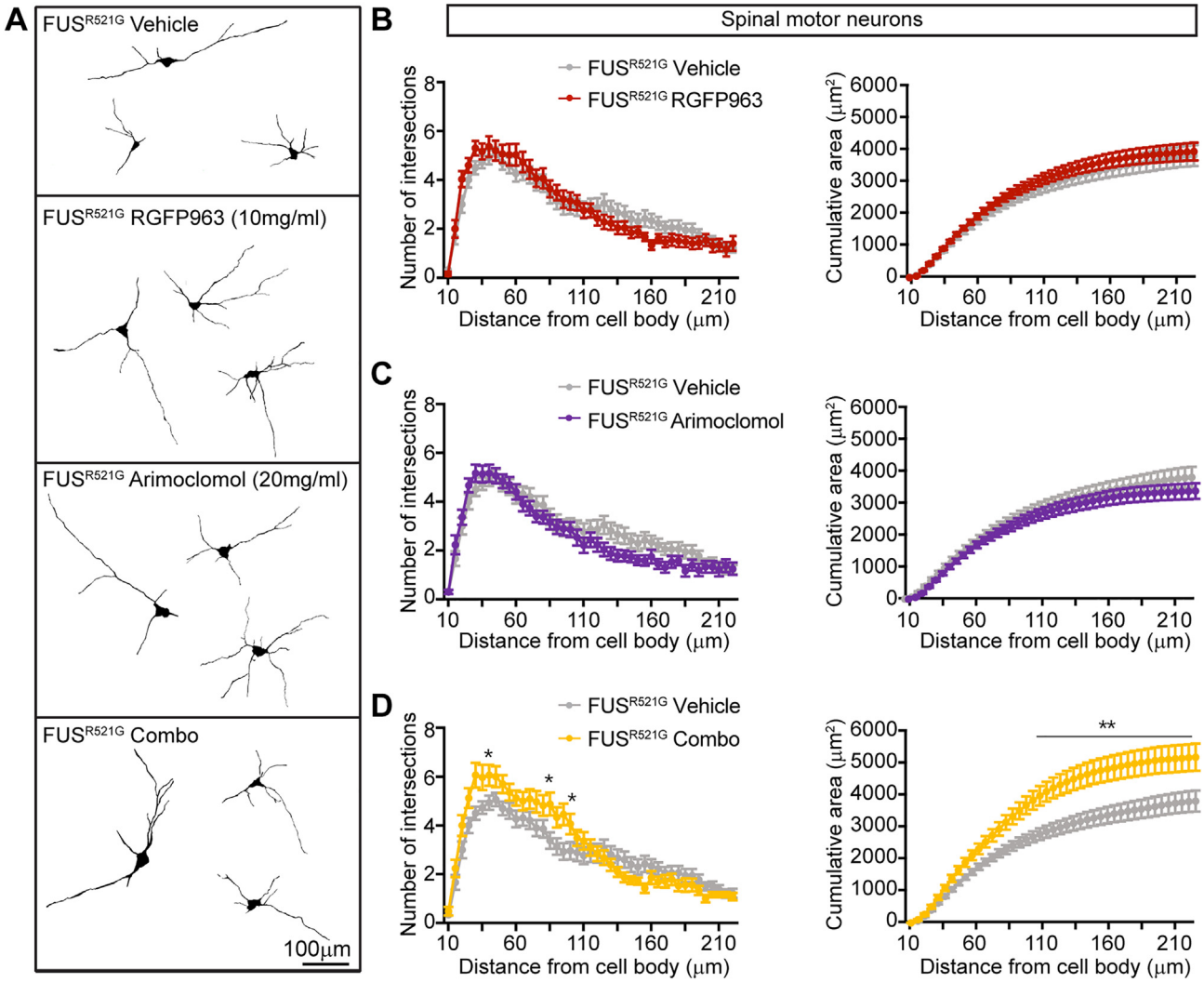

Fig. 3. Combination treatment improved dendritic branching of spinal motor neurons. (A) Neurolucida tracing of spinal motor neurons from FUS^{R521G} mice treated with vehicle, 10 mg/kg RGFP963, 20 mg/kg arimoclomol or the combination. Sholl analysis showing no significant changes in dendritic intersections and cumulative area of dendrites in (B) RGFP963- or (C) arimoclomol-treated mice, but a significant increase in dendritic branching and cumulative area in mice treated with (D) the drug combination. Values from each group are represented as mean ± SEM. Statistical analysis was by two-way repeat measures ANOVA with Bonferroni correction test for Sholl analysis (n = 3 mice/group). *$p < 0.05$, **$p < 0.01$.

including HSF1 as well as protein chaperoning, and HSPB1, which serves as a 'holdase' to sequester misfolded proteins (Fig. 5, Fig. 6 and Fig. S4). Neither expression of FUS^{R521G} nor treatment with RGFP963, arimoclomol or the drug combinations resulted in any significant change in HSP levels in cortex (Fig. 5) or gastrocnemius/soleus muscle (Fig. 6). In addition, there were no changes in cortical levels of HSF1 or appearance of bands with higher apparent molecular weight indicative of HSF1 phosphorylation associated with transcriptional activation (Fig. S5).

Thus, the dramatic reversal of cognitive impairment and improvement in dendritic architecture observed with drug treatments in FUS^{R521G} mice were not attributable to increase in HSP expression.

Effect of drug treatments on expression of HSPs and neuromuscular function at various disease stages in SOD1^{G93A} transgenic mice

In the Gurney line of SOD1^{G93A} transgenic mice, 10 mg/kg arimoclomol delayed motor neuron loss and muscle denervation and prolonging lifespan, increasing HSF1 phosphorylation and expression of HSP70 and HSP90 in spinal cords at late-stage disease [8,19]. In cultured motor neurons expressing SOD1^{G93A}, we found induction of HSPA1A to be minimal, but some enhancement was obtained by treatment with arimoclomol or HDAC inhibitors [12,15,16]. We therefore conducted a more comprehensive analysis of HSP expression in SOD1^{G93A} transgenic mice at different stages of disease for comparison to the FUS ALS models.

In this line of SOD1^{G93A} mice, motor neuron loss becomes evident by P90, although deficits of neuromuscular innervation and function are measurable by P30 [9,25,26]. Subsequently, mice exhibit abnormal hindlimb splay reflex followed quickly by paralysis around P120. Mice were treated with vehicle, 20 mg/kg arimoclomol, 10 or 20 mg/kg RGFP963 or the drug combination using three regimens: from P50-P75 to evaluate early deficits in neuromuscular function; from P75-P105 to encompass the early symptomatic stage; and from P105 to endstage to encompass the late symptomatic stage of disease. Levels of HSPs in homogenates of lumbar spinal cord and skeletal muscle (gastrocnemius/soleus) were quantified by Western analysis.

At P105, no changes in HSPA1A, HSPA8, HSP40 or HSP90 were measured in spinal cord of SOD1^{G93A} mice relative to littermate controls, nor with drug treatments (Fig. S6). On the other hand, multiple HSPs (HSPA1A, HSPA8, HSP40 and STIP1 (a.k.a. HOP, an adapter protein coordinating HSP70 and HSP90 functions)) were upregulated in gastrocnemius/soleus muscle, with drug treatments having minimal effect (Fig. 7). HSPB1 was upregulated in astrocytes of lumbar spinal cord

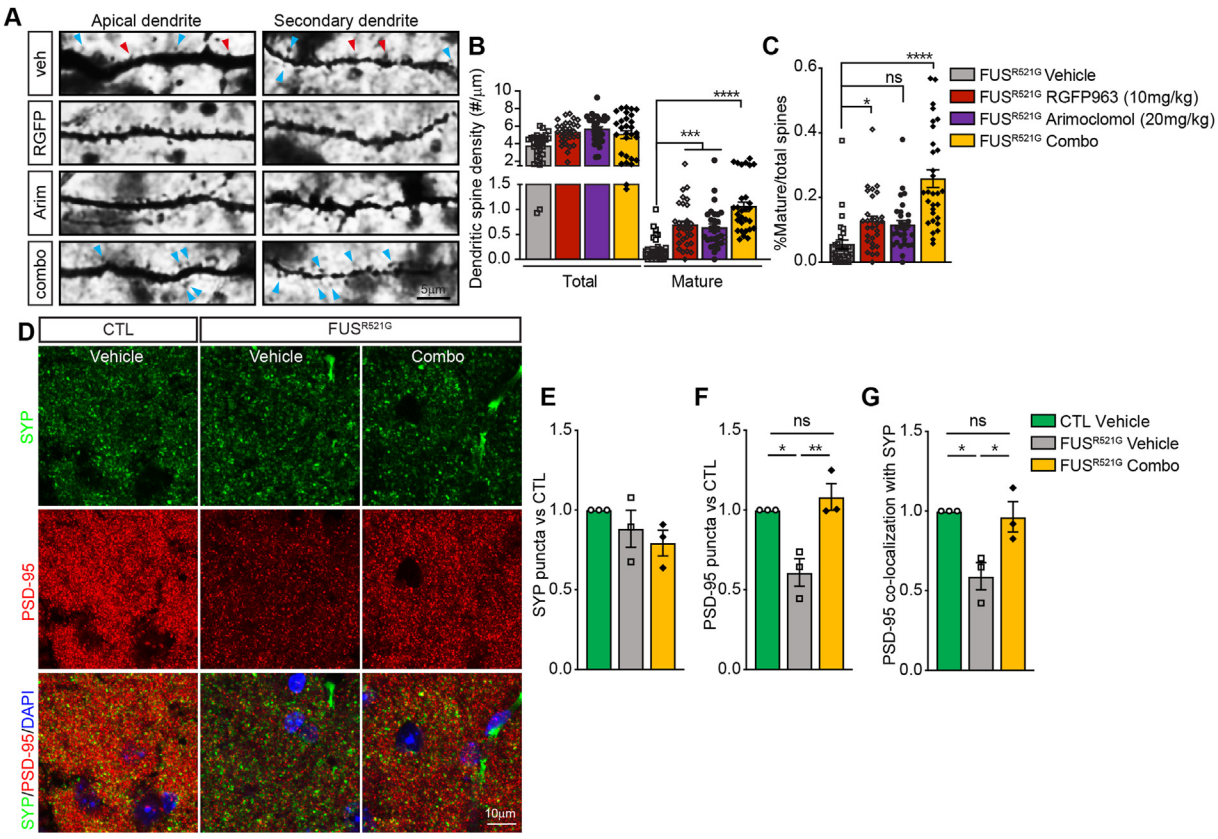

Fig. 4. RGFP963 and arimoclomol improved dendritic spine densities in cortex of FUS^{R521G} mice. (A) Golgi images of dendritic spines on cortical neurons in FUS^{R521G} treated with vehicle (veh), 10 mg/kg RGFP963 (RGFP), 20 mg/kg arimoclomol (Arim) or the drug combination (combo) and (B, C) their quantification. (B) Increase in overall dendritic spine density and (C) the percentage of mature spines in mice treated with RGFP963, arimoclomol or the combination compared to vehicle-treated mice. (D) Co-labelling of cortex of FUS^{R521G} and littermate control (CTL) mice with the pre-synaptic marker anti-synaptophysin (SYP), the post-synaptic marker anti-PSD-95 and DAPI (nuclear marker), showing significant reduction in synaptic density in FUS^{R521G} cortex. Treatment with the drug combination resulted in no changes in the pre-synapse as determined by the number of (E) SYP puncta, but significant increase in (F) PSD-95 puncta. (G) Increased co-localization of PSD-95 with SYP in cortex of mice treated with the drug combination compared to vehicle-treated FUS^{R521G} mice. Values from each group are expressed as mean ± SEM. Statistical analysis was by one-way ANOVA with Tuckey correction to determine significance and an unpaired Student's *t*-test for comparison between two groups (n = 3–4 mice/group). *p < 0.05, **p < 0.01, ***p < 0.005 ****p < 0.001, and not significant (ns). Red and blue arrows indicate immature and mature spines, respectively.

as previously reported [12,27] and in gastrocnemius/soleus muscle, both at P105 and more extensively at endstage (Fig. S7).

At endstage disease, levels of HSPA1A, HSPA8, HSP40, HSP90 and STIP1 remained unchanged in lumbar spinal cord of SOD1^{G93A} mice relative to littermate controls (Fig. 7, Fig. S9). All drug treatments significantly increased the level of HSPA8, but not the other HSPs, relative to vehicle-treated mice. Levels of all HSPs were substantially increased in skeletal muscle of SOD1^{G93A} mice but were not further increased by drug treatments. Rather levels decreased, particularly in mice treated with the combination of RGFP963 and arimoclomol (Fig. 8).

Effect of drug treatments on body weight and motor behavioral testing in SOD1^{G93A} mice

Clinical disease was evaluated in P75-P105 and P105-endstage treatment groups by loss of body weight and deterioration in performance on behavioral measures of motor function (Fig. S10). At P105, there was no significant change in body weight among groups (Fig. S10A), but latency to fall in the hanging wire test was impaired in SOD1^{G93A} mice compared to nontransgenic littermates (Fig. S10C). Only the combination treatment resulted in minor but significant reduction in this impairment. At endstage, body weight was significantly reduced in SOD1^{G93A} mice (Fig. S10B), but this loss was not prevented by any treatment. Treatments also failed to prevent impairment on the hanging wire test (Fig. S10D) or reduced grip strength (Fig. S10E).

Thus, the only significant effect of treatment on motor function was in the P75-P105 cohort in which combination treatment produced a minor delay in impairment on the hanging wire test. Since impairment in physiological measurements of neuromuscular function are well documented at earlier stages of disease, mice were treated with vehicle, 20 mg/kg RGFP963, 20 mg/kg arimoclomol or the drug combination from P50 to P75 to determine if treatments might show better improvement at this stage.

Drug treatments result in modest improvement in muscle contractile force, but not innervation in SOD1^{G93A} mice at P75

Motor function was assessed through behavioral tests for prehensile force (Grip Strength Test) (Fig. S11A), motor coordination (Rotarod) (Fig. S11B) and endurance (Hang Time) (Fig. S11C), but at the end of the 3-week treatment, no significant impairment on these motor tests resulted from expression of the transgene, as expected at this stage, nor by any drug treatment. On the other hand, structural and functional neuromuscular defects are well documented in SOD1^{G93A} mice at this age. At the end of treatment, neuromuscular properties were investigated in EDL muscles isolated with a segment of the deep fibular nerve and mounted as shown in Fig. S11D. The nerve and the muscle were stimulated sequentially at frequencies ranging from 5 to 300 Hz and the force generated by the muscle contraction was recorded on a force transducer (Fig. S11E). With all experimental paradigms, SOD1^{G93A} mice were

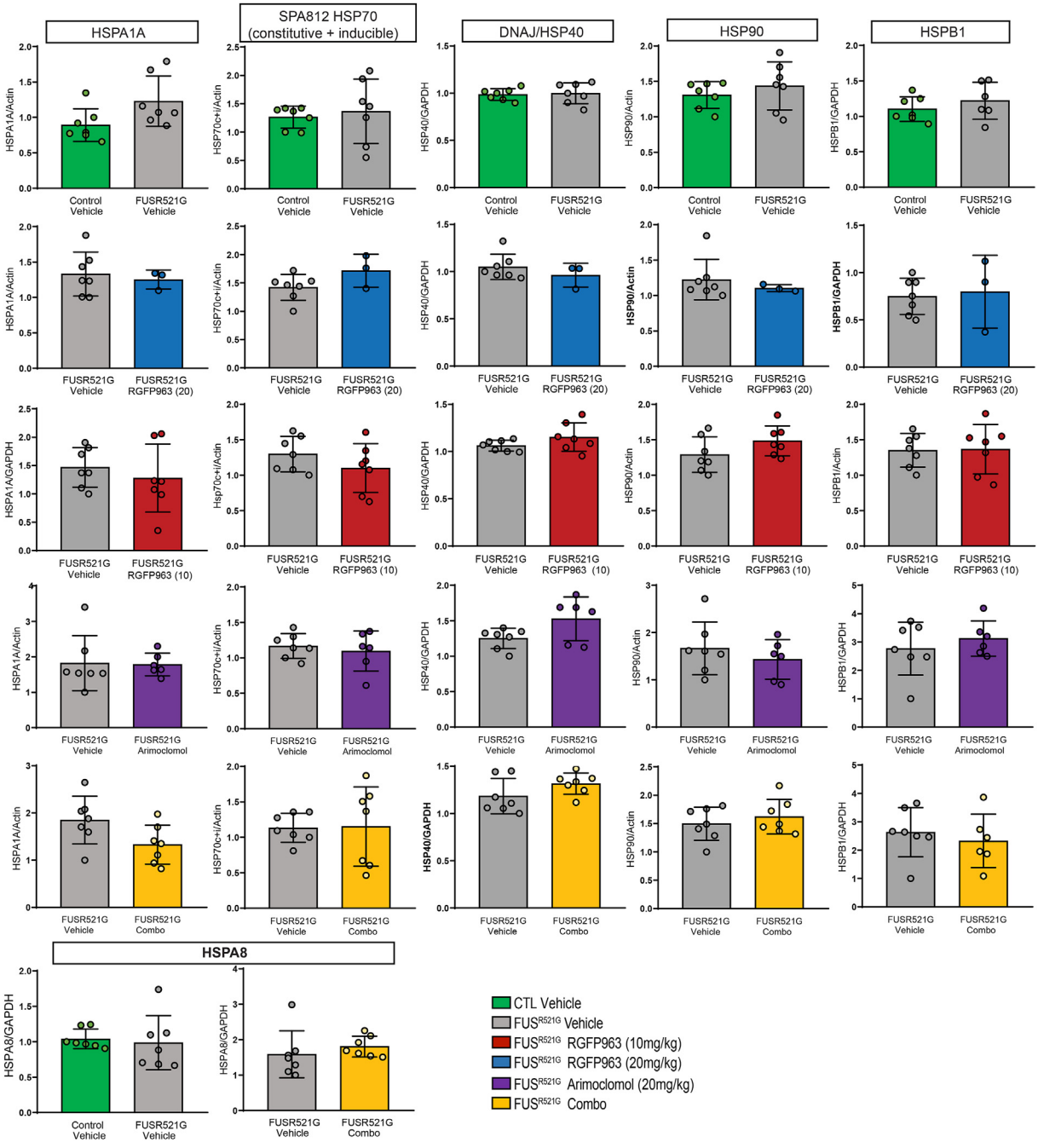

Fig. 5. No significant change in expression of HSP70 isoforms, HSP40, HSP90 or HSPB1 in FUS^{R521G} cortex or with drug treatments. FUS^{R521G} mice were treated daily *i.p.* for 28 days beginning on P60 with vehicle, 20 mg/kg RGFP963, 10 mg/kg RGFP963), 20 mg/kg arimoclomol or the combination. Western blots of homogenates of cortex were probed with antibodies smc-100 (HSPA1A), SPA812 (inducible and constitutive HSP70), smc-151 (HSPA8), ADI-SPA-400 (HSP40), smc-149 (HSP90) or sc-1049 (HSPB1) and normalized to GAPDH or actin. Top row: Levels of HSPs were unchanged in cortex of FUS^{R521G} compared to control mice. Rows 2–5: Levels were not affected by any drug treatments. Data are shown as mean ± SD (3–7 mice/group). Statistical analysis was by unpaired, two-tailed Student's *t*-test; $*p < 0.05$, $**p < 0.01$, $***p < 0.001$.

impaired relative to nontransgenic littermates. Nerve stimulation in the 80–250 Hz range generated more force in EDLs from arimoclomol-treated SOD1^{G93A} mice compared to EDLs from vehicle-treated SOD1^{G93A} mice (Fig. S11F). Interestingly, more force was generated in that stimulation range by direct muscle stimulation in all treated groups compared to vehicle-treated SOD1^{G93A} mice, as well as in EDLs from arimoclomol- and RGP963-treated mice stimulated at 40 Hz (Fig. S11G).

Next, fatigue was induced by rapid, successive 120 Hz stimulation for 180 s. The force generated by the EDLs at the end of the fatigue protocol was similar across all SOD1^{G93A} groups, with the exception that direct muscle stimulation of EDLs from mice treated with the drug combination generated more contractile force compared to vehicle treatment (Figs. S11H and I). All muscles recovered at least 90% of their original force in the 30 min following the fatigue protocol.

The integrity of the NMJs of these EDLs was assessed as in FUS^{R521G} mice by quantifying the overlap between markers of the pre-synaptic terminals (NFM and synaptic vesicle protein 2 (SV2)) and the post-synaptic receptors (α-bungarotoxin) (Fig. S11J). Over half of EDLs from all groups of SOD1^{G93A} mice were denervated compared to EDLs from nontransgenic littermates, but there were no significant differences in the

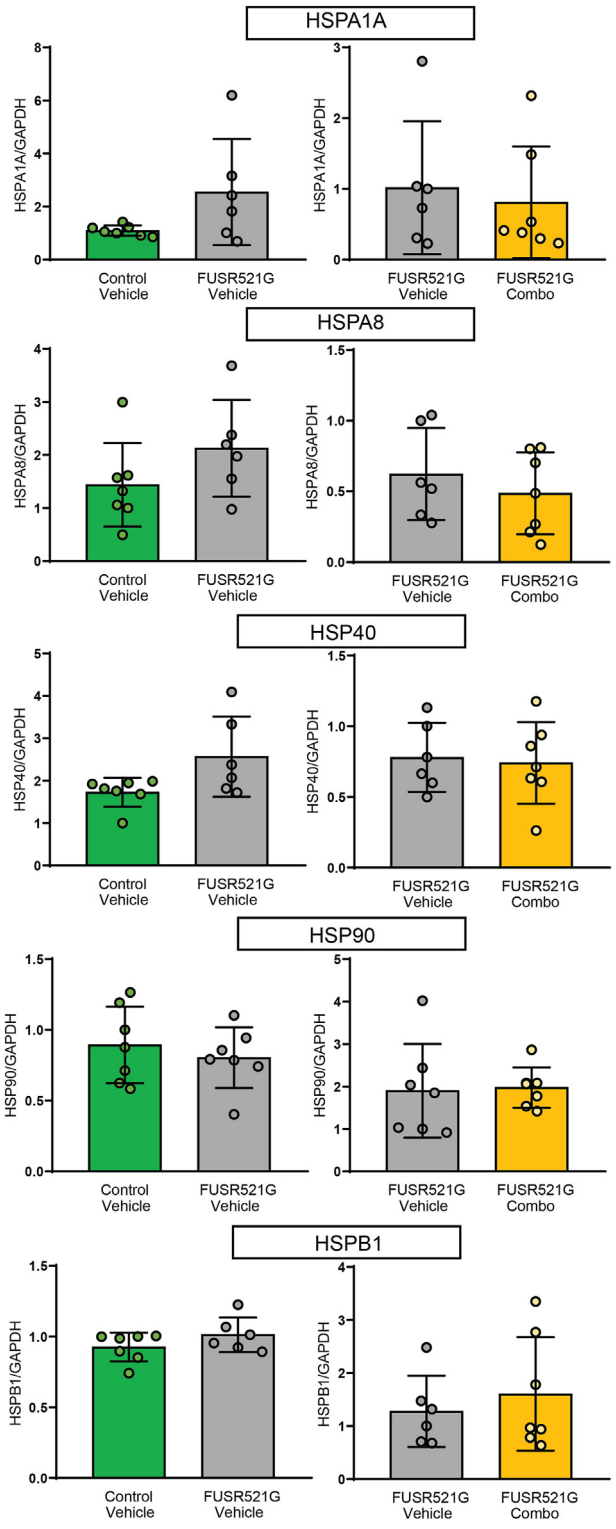

Fig. 6. No change in expression of heat shock proteins in gastrocnemius/soleus muscle of FUS^{R521G} mice or with drug treatments. FUS^{R521G} mice were treated for 28 days (7 days/week) *i.p.* beginning P60 with vehicle or the combination of 20 mg/kg arimoclomol and 10 mg/kg RGFP963. Homogenates of muscles were analyzed for levels of HSPA1A, HSPA8, HSP40, HSP90 or HSPB1 by Western blotting and normalized to GAPDH. Levels of HSPs were unchanged in muscles of FUS^{R521G} compared to control mice (left column). Combination treatment had no effect on their levels (right column). Data are presented as mean ± SD (7 mice/group). Statistical analysis was by unpaired, two-tailed Student's *t*-test; $*p < 0.05$, $**p < 0.01$, $***p < 0.001$.

proportion of completely denervated NMJs among the $SOD1^{G93A}$ treatment groups (Fig. S11K).

Thus, drug treatments produced significant, although modest, improvement in skeletal muscle contractile force in $SOD1^{G93A}$ mice, but without sustaining NMJ innervation.

Discussion

Approximately 10% of ALS cases are familial with over 40 identified genes showing disease association (ALSoD). These genes encode proteins involved in several categories of biological processes including DNA/RNA binding, RNA processing, intracellular transport, metabolic processes, and protein quality control [28]. *SOD1* was the first ALS gene identified and cellular and animal models have served as major tools to identify disease mechanisms and potential therapeutic approaches [17]. Although SOD1 is an antioxidant enzyme, gain of toxic function rather than loss of dismutase activity causes motor neuron disease. Mutations result in abnormal protein conformation leading to inappropriate interactions and aggregation, with numerous downstream consequences. Formation of protein aggregates is a common feature among different forms of familial ALS as well as sporadic disease of unknow cause, pointing to failure of mechanisms of protein quality control as a central and common factor of pathogenesis to target therapeutically.

Whereas SOD1 mutations cause a predominant motor phenotype in patients and mouse models, mutations in RNA binding protein genes (*e.g., TARDBP*, *FUS*, *HNRNPA1*) and hexanucleotide expansion in *C9ORF72* can result in a spectrum of presentation from motor neuron disease to frontotemporal dementia. Both presentations are modeled in the mice expressing the human FUS^{R521G} variant used in this study; they develop severe cognitive deficits as well as motor impairment, compared to the predominant motor neuron disease in mice overexpressing human SOD1 variants. Mild cognitive impairment and learning disability have been reported in some pediatric patients with *FUS* mutation [29,30].

As in our culture model of ALS-FUS^{R521G}, both arimoclomol and the HDAC inhibitor RGFP963 were neuroprotective in FUS^{R521G} mice without enhancing expression of HSPs. The mice showed severe deficits in novel object recognition and passive avoidance tests before drug treatment was initiated. Surprisingly, these deficits were reversed in a dose-dependent fashion by arimoclomol and by RGFP963 treatment. The increase in the number and density of mature dendritic spines on cortical neurons points to a general recovery of synaptic integrity that could be a contributing factor to this recovery. FUS plays many roles in RNA processing including RNA splicing, transport of mRNAs to neuronal processes, local translation and maintenance of synaptic connections [31]. The mechanism(s) underlying recovery with arimoclomol treatment is unlikely related to its putative role as an amplifier of the heat shock response. Indeed, consistent with results in cultured motor neurons [15,16], there were no increases in expression of a battery of HSPs with complementary function (HSPA1A, HSPA8, HSP40, HSPB1, HSP90 or STIP1/HOP) in spinal cord, cortex or skeletal muscle of FUS^{R521G} mice, nor in these mice treated with arimoclomol, RGFP963 or the combination. Nor was there evidence of change in level or activation of the transcription factor HSF1.

Arimoclomol was previously reported to delay motor neuron loss and muscle denervation in $SOD1^{G93A}$ mice and to increase HSF1 phosphorylation and expression of HSP70 and HSP90 in spinal cords at late-stage disease [8,19]. We studied these mice in comparison to the FUS^{R521G} mice. Unlike in FUS mice, upregulation of multiple HSPs was evident in skeletal muscle at intermediate stage disease, being more pronounced at endstage. However, no upregulation was evident in lumbar spinal cord, other than HSPB1 associated with astrocytosis, nor was enhancement observed with any drug treatment regimen; rather, HSP levels were less pronounced in skeletal muscle, suggesting that other protective mechanisms reduced the need for the additional HSPs. Indeed, muscle contractile force was increased by drug treatments.

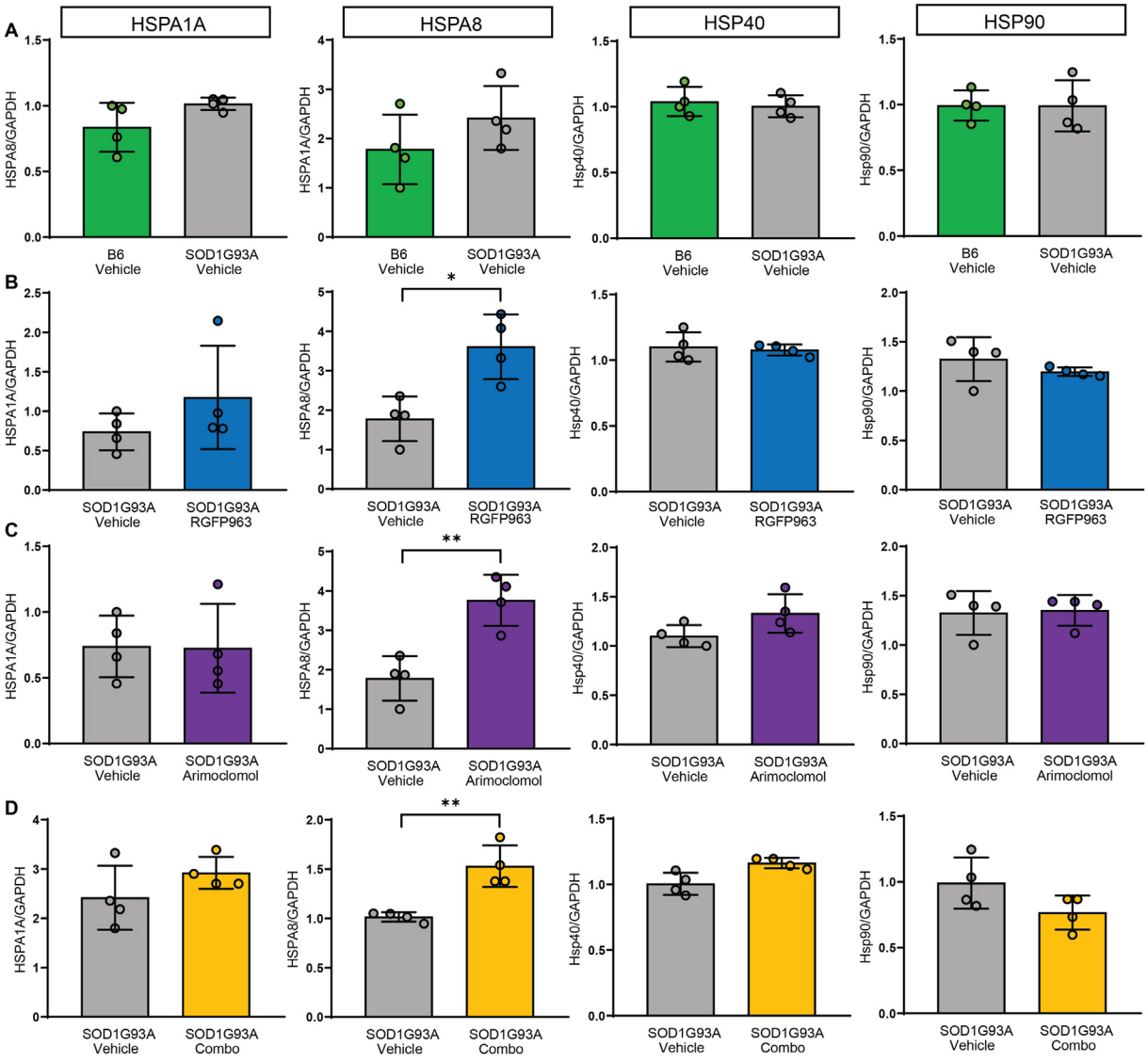

Fig. 7. Drug treatments increased only HSPA8 in lumbar spinal cord (LSC) of endstage SOD1^{G93A} mice. B6 nontransgenic and SOD1^{G93A} transgenic mice were treated 5 days/week *i.p.* from P85 to endstage with vehicle, 20 mg/kg RGFP963, 20 mg/kg arimoclomol, or the combination. Homogenates of LSC were analyzed for levels of HSPA1A, HSPA8, HSP40 and HSP90 by Western blotting and normalized to GAPDH. (A) HSP levels were unchanged in LSC from SOD1^{G93A} mice compared to B6 control mice. (B–D) HSPA8 levels were significantly elevated by drug treatments, but HSPA1A, HSP40 and HSP90 remained unchanged. Data are shown as mean ± SD (4 mice/group). Statistical analysis was by unpaired, two-tailed Student's *t*-test; $^{*}p < 0.05$, $^{**}p < 0.01$, $^{***}p < 0.001$.

Consistent with results in fALS culture models, activation of the conventional heat shock response in motor neurons varies with the type of stress [12,15,16,32]. Proteasome inhibitors do upregulate the stress-inducible isoform HSPA1A, but the transcription factor HSF2, which accumulates when the proteasome is sufficiently inhibited, could be involved [12]. In mouse models of disease, the response can be even more variable and refractory, as illustrated by the following examples. The HSP90 inhibitor NXD30001was highly effective in increasing HSPA1A in cultured motor neurons, but not in the SOD1^{G93A} mouse model, even in peripheral tissues [5]. In *NPC1*$^{-/-}$ mice, a model of the lysosomal storage disease Niemann-Pick Type C, arimoclomol increased HSF1 phosphorylation and restored HSP70 levels in brain, but not in liver. In mice expressing humanized valosin-containing protein (VCP/p97) with the dominant mutation A232E causing a multisystem disorder of nervous system, bone and muscle, HSP70 was increased almost 3-fold in motor neurons compared to wild type controls and further increased by treatment with 120 mg/kg arimoclomol [33]. In skeletal muscle HSP70 was not elevated by the variant but was enhanced by arimoclomol [33]. Notably, arimoclomol was administered *p.o.* with an estimated dosage of 120 mg/kg compared to the maximum dosage of 20 mg/kg *i.p.* in our study. Regardless, the reversal of cognitive deficit in the ALS-FUS mice occurred without evidence of HSP induction or reduction in FUS expression (Fig. S12). Neither FUS levels nor solubility in cortex of ALS-FUS mice were significantly altered by arimoclomol treatment (Fig. S12A). Accumulation of insoluble FUS is not a feature of the FUS^{R521G} line used in this study (Fig. S12B). Thus, the phenotype is similar to the mouse developed by Huang, which also expresses FUS at similar levels as control mice and experiences defects in memory and spatial awareness [21]. On the other hand, RGFP963 treatment increased cortical FUS. Further study would be required to understand the mechanism, epigenetic alteration in FUS expression or direct interaction of HDACs with FUS being possibilities [34,35].

How FUS variants suppress the heat shock response remains unknown. Epigenetic mechanisms regulating HSP gene expression could be involved but were not overcome by HDAC inhibition to promote active chromatin or by maintaining nBAF chromatin remodeling complexes in the nucleus [15], both important for HSF1 interaction with HSE [36]. HDAC inhibition would impact other protective mechanisms, including

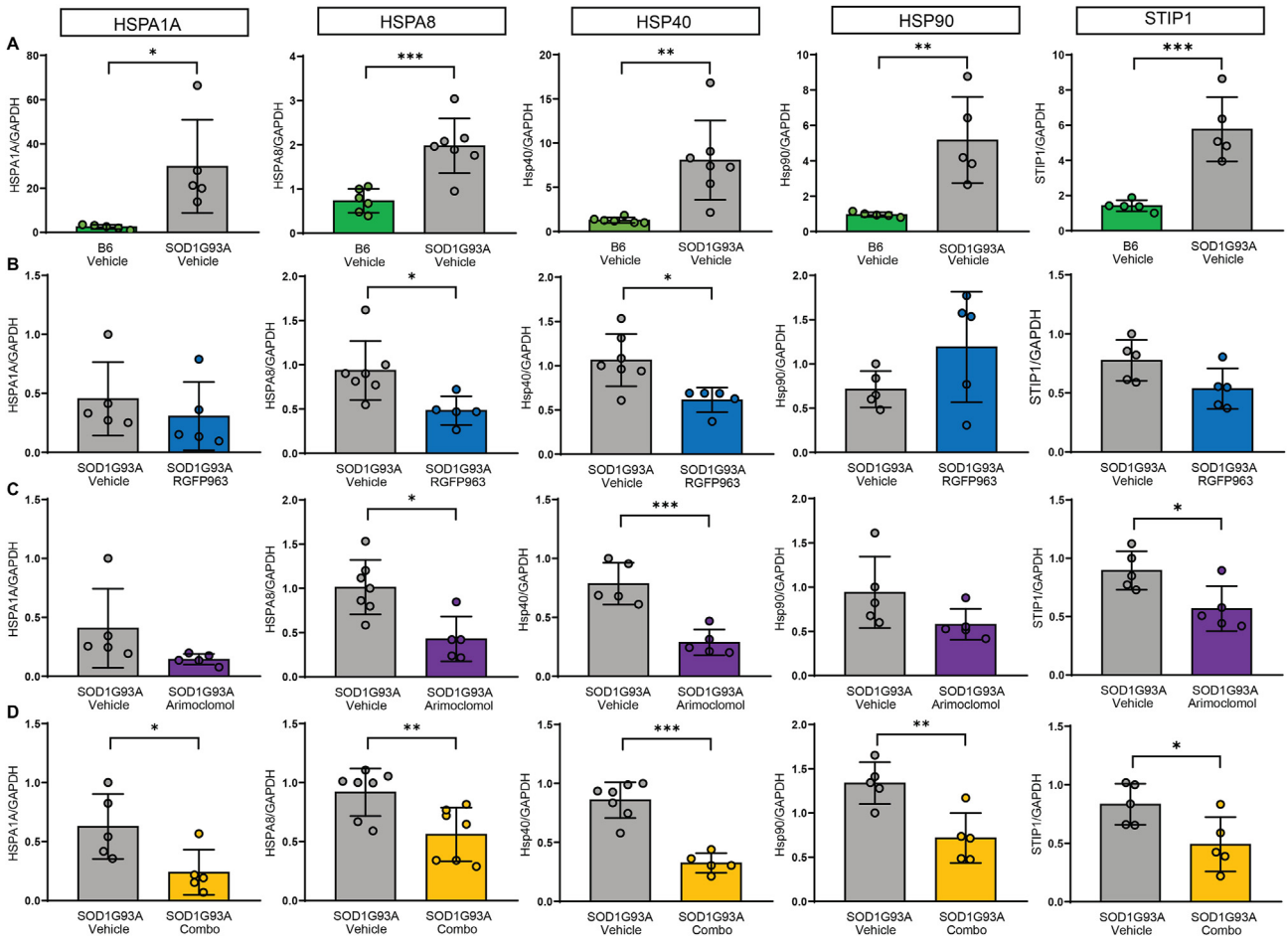

Fig. 8. Increase in HSPA1A, HSPA8, HSP40, HSP90 and STIP1/HOP in gastrocnemius/soleus muscle of endstage SOD1^{G93A} mice, but no augmentation by drug treatments. B6 nontransgenic and SOD1^{G93A} mice were treated 5 days/week *i.p.* from P85 to endstage with vehicle, 20 mg/kg RGFP963, 20 mg/kg arimoclomol or the combination. Homogenates of gastrocnemius/soleus were analyzed for HSPA1A, HSPA8, HSP40, HSP90 or STIP1/HOP by Western blotting and normalized to GAPDH. (A) Levels of HSPA1A, HSPA8, HSP40, HSP90 and STIP1 were increased in muscle from SOD1^{G93A} mice compared to B6 control mice. (B-D) Combination drug treatment significantly reduced the elevation in HSP levels. Data are shown as mean ± SD (5–7 mice/group). Statistical analysis was by unpaired, two-tailed Student's *t*-test; $^{*}p < 0.05$, $^{**}p < 0.01$, $^{***}p < 0.001$.

DNA repair [15]. Arimoclomol was screened for binding of representative classical receptors, transporters and ion channels, and various kinases, and found to interact with FGR kinases, MAPKAPK2, PRKACA and GSK3β [37], pointing to other potential pathways. GSK3β was particularly interesting, being an important signaling molecule for cell survival and memory. Phosphorylation (pGSK3β) inactivates the kinase by promoting proteasome degradation. pGSK3β is substantially reduced in neurodegenerative disease including ALS, leading to increased activity with harmful downstream consequences to neuronal maintenance and metabolic processes [38]. Levels were reduced in the cortex of FUS^{R521G} mice, but treatment with arimoclomol or RGFP963 had no significant effect (data not shown).

Although focus for developing therapeutics has been on increasing the amount of HSPs to combat protein misfolding, the level might not be the only or even major limiting factor for protein quality control during stress in neurons [39,40]. HSPs need to be in the right place, in particular to protect synaptic connections. Chen and Brown reported that constitutively expressed HSC70 was translocated to synaptic areas of rabbit cerebral cortex after thermal stress, to promote protein folding in association with HSP40 [41]. Neurons normally express high levels of constitutive HSPs including HSPA8 [11,39]. Indeed, *Hspa8* mRNA is the most abundant dendritic chaperone and local translation efficiency is enhanced by proteotoxic stress [32]. Given that attrition of motor neuron dendrites is a common theme in ALS [42,43], compromise of proximal connections as well as neuromuscular junctions would contribute to motor impairment. Consistent with this, localization of *Hspa8* mRNA to dendrites was impaired in cultured murine motor neurons expressing FUS^{R521G} and in neurons derived from human induced pluripotent stem cells expressing a pathogenic variant of heterogenous nuclear ribonucleoprotein A2/B1 [32]. *Hspa8* mRNA levels were reduced in soma and dendrites of cultured motor neurons expressing FUS^{R521G}, but not restored by arimoclomol or HDAC inhibition [16]. Levels of *Hspa8* mRNA and protein were reduced in motor neurons expressing ALS variants of SOD1, TDP-43 and FUS indicating multiple compromises in chaperoning capacity. Treatments had variable, often different effects on expression and intracellular distribution of *Hspa8* mRNA depending on the ALS variant, and on biomarkers of toxicity, further highlighting the need to understand the function of different ALS variants to better tailor therapeutic approaches.

At this time, we can't say how the counteraction of cognitive impairment by arimoclomol or HDAC inhibition applies across the various types of ALS. Recently, there has been awareness of cognitive involvement in patients with *SOD1* mutation, particularly in language domains and social cognition [44]. Assessment of cognitive performance was not planned in the SOD1^{G93A} mice in this study, as it was not a usual or expected endpoint in high copy number SOD1^{G93A} transgenic mice, given the profound motor phenotype. Also, the mice obtained from JAX have developed a hyperkinetic behavior, independent of the classic motor deficits, and they were difficult to handle for behavioral testing. In the phase III clinical trial of arimoclomol in sporadic ALS, cognitive testing was not listed as an

outcome measure. The outcome measures were: Time from baseline to one of the events (PAV/tracheostomy/death), ALSFRS-R and Slow Vital Capacity. Thus, there would be limited ability to identify participants with deficits or benefiting from therapy [10].

Overall, the study reinforces the challenges in therapeutic development in a complex family of diseases called ALS. Disease mechanisms can differ with the initiating factor(s) and stage of disease. In drug trials, it is important to measure multiple endpoints and target engagement, but also to be attuned to 'off target' effects, which can significantly impact outcomes and interpretation of results.

Author Contributions

Heather Durham, and Josephine Nalbantoglu conceived the study. Heather Durham, Josephine Nalbantoglu, Chantelle Sephton and Richard Robitaille designed the study, obtained funding, supervised the research, analyzed data and played the major roles in drafting the manuscript. Mari Pelaez, Frédéric Fiore, Nancy Larochelle and Danielle Arbour assisted with writing and editing the manuscript. Mari Pelaez, Nancy Larochelle, Frédéric Fiore, Afrooz Dabbaghizadeh, Mario Fernández Comaduran, Danielle Arbour, Sandra Minotti, Laetitia Marcadet and Martine Semann collected and analyzed data.

Ethics approval

All experimental procedures were approved by the Institutional Animal Care Committees of the McGill University, Université Laval and Université de Montréal and carried out in accordance with the Canadian Council on Animal Care.

Declaration of competing interest

The authors declare the following financial interests/personal relationships which may be considered as potential competing interests: Heather Durham reports financial support was provided by Merck, Sharpe & Dohme Corporation, McGill Faculty of Medicine. Heather Durham reports financial support was provided by Brain Canada Foundation and ALS Society of Canada. Heather Durham reports equipment, drugs, or supplies was provided by BioMarin Pharmaceutical Inc. Chantelle Septhton reports financial support was provided by Brain Canada Foundation and ALS Society of Canada and FRSQ. Mario Fernandez Comaduran reports financial support was provided by Fonds de Recherche du Québec Nature et Technologies and Mitacs Globalink Graduate Fellowship, Consejo Nacional de Ciencia y Tecnología. If there are other authors, they declare that they have no known competing financial interests or personal relationships that could have appeared to influence the work reported in this paper.

Funding and acknowledgements

This study was supported by an ALS Canada-Brain Canada Hudson Translational Team Grant (HDD, JN, CFS and RR) provided by Brain Canada through the Canada Brain Research Fund with the financial support of Health Canada and the ALS Society of Canada, and by a Merck, Sharpe & Dohme Corporation/McGill Faculty of Medicine Grant for Translational Research (HDD, JN). CFS was supported by ALS Canada–-Brain Canada Career Transition Award and Fonds de Recherche du Québec Santé Junior 1. MFC was supported by Fonds de Recherche du Québec Nature et Technologies and Mitacs Globalink Graduate Fellowship, Consejo Nacional de Ciencia y Tecnología. RGFP963 was a kind gift of BioMarin Pharmaceutical Inc., San Raphael, CA USA.

Appendix A. Supplementary data

Supplementary data to this article can be found online at https://doi.org/10.1016/j.neurot.2024.e00388.

References

[1] Morimoto RI, Sarge KD, Abravaya K. Transcriptional regulation of heat shock genes. J Biol Chem 1992;267:21987–90.
[2] Kmiecik SW, Mayer MP. Molecular mechanisms of heat shock factor 1 regulation. Trends Biochem Sci 2022;47(3):218–34.
[3] Ali A, Bharadwaj S, Ocarroll R, Ovsenek N. HSP90 interacts with and regulates the activity of heat shock factor 1 in xenopus oocytes. Mol Cell Biol 1998;18:4949–60.
[4] Batulan Z, Taylor DM, Aarons RJ, Minotti S, Doroudchi MM, Nalbantoglu J, et al. Induction of multiple heat shock proteins and neuroprotection in a primary culture model of familial amyotrophic lateral sclerosis. Neurobiol Dis 2006;24(2):213–25.
[5] Cha JR, St Louis KJ, Gentil BJ, Tibshirani M, Tradewell ML, Jaffer ZM, et al. A novel small molecule HSP90 inhibitor, NXD30001, differentially induces heat shock proteins in nervous tissue in culture and in vivo. Cell Stress Chaperones 2014;19:421–35.
[6] Labbadia J, Cunliffe H, Weiss A, Katsyuba E, Sathasivam K, Seredenina T, et al. Altered chromatin architecture underlies progressive impairment of the heat shock response in mouse models of Huntington disease. J Clin Invest 2011;121(8):3306–19.
[7] Hargitai J, Lewis H, Boros I, Racz T, Fiser A, Kurucz I, et al. Bimoclomol, a heat shock protein co-inducer, acts by the prolonged activation of heat shock factor-1. Biochem Biophys Res Commun 2003;307(3):689–95.
[8] Kieran D, Kalmar B, Dick JR, Riddoch-Contreras J, Burnstock G, Greensmith L. Treatment with arimoclomol, a coinducer of heat shock proteins, delays disease progression in ALS mice. Nat Med 2004;10(4):402–5.
[9] Kalmar B, Novoselov S, Gray A, Cheetham ME, Margulis B, Greensmith L. Late stage treatment with arimoclomol delays disease progression and prevents protein aggregation in the SOD1 mouse model of ALS. J Neurochem 2008;107(2):339–50.
[10] Benatar M, Hansen T, Rom D, Geist MA, Blaettler T, Camu W, et al. Safety and efficacy of arimoclomol in patients with early amyotrophic lateral sclerosis (ORARIALS-01): a randomised, double-blind, placebo-controlled, multicentre, phase 3 trial. Lancet Neurol 2024;23:687–99.
[11] Manzerra P, Brown IR. Expression of heat shock genes (hsp70) in the rabbit spinal cord: localization of constitutive and hyperthermia-inducible mRNA species. J Neurosci Res 1992;31:606–15.
[12] Batulan Z, Shinder GA, Minotti S, He BP, Doroudchi MM, Nalbantoglu J, et al. High threshold for induction of the stress response in motor neurons is associated with failure to activate HSF1. J Neurosci 2003;23(13):5789–98.
[13] Guertin MJ, Lis JT. Chromatin landscape dictates HSF binding to target DNA elements. PLoS Genet 2010;6(9):e1001114.
[14] Tibshirani M, Tradewell ML, Mattina KR, Minotti S, Yang W, Zhou H, et al. Cytoplasmic sequestration of FUS/TLS associated with ALS alters histone marks through loss of nuclear protein arginine methyltransferase 1. Hum Mol Genet 2015;24(3):773–86.
[15] Kuta R, Larochelle N, Fernandez M, Pal A, Minotti S, Tibshirani M, et al. Depending on the stress, histone deacetylase inhibitors act as heat shock protein co-inducers in motor neurons and potentiate arimoclomol, exerting neuroprotection through multiple mechanisms in ALS models. Cell Stress Chaperones 2020;25(1):173–91.
[16] Fernandez Comaduran M, Minotti S, Jacob-Tomas S, Rizwan J, Larochelle N, Robitaille R, et al. Impact of histone deacetylase inhibition and arimoclomol on heat shock protein expression and disease biomarkers in primary culture models of familial ALS. Cell Stress & Chaperones 2024;29:359–80.
[17] Gurney ME, Pu H, Chiu AY, Dal Canto MC, Polchow CY, Alexander DD, et al. Motor neuron degeneration in mice that express a human Cu, Zn superoxide dismutase mutation. Science 1994;264:1772–5.
[18] Sephton CF, Tang AA, Kulkarni A, West J, Brooks M, Stubblefield JJ, et al. Activity-dependent FUS dysregulation disrupts synaptic homeostasis. Proc Natl Acad Sci U S A. 2014;111(44):E4769–78.
[19] Kalmar B, Edet-Amana E, Greensmith L. Treatment with a coinducer of the heat shock response delays muscle denervation in the SOD1-G93A mouse model of amyotrophic lateral sclerosis. Amyotroph Lateral Scler 2012;13(4):378–92.
[20] Pelaez MC, Desmeules A, Gelon PA, Glasson B, Marcadet L, Rodgers A, et al. Neuronal dysfunction caused by FUSR521G promotes ALS-associated phenotypes that are attenuated by NF-κB inhibition. Acta Neuropathol Commun 2023;11(1):182.
[21] Qiu H, Lee S, Shang Y, Wang WY, Au KF, Kamiya S, et al. ALS-associated mutation FUS-R521C causes DNA damage and RNA splicing defects. J Clin Invest 2014;124(3):981–99.
[22] Ho WY, Agrawal I, Tyan SH, Sanford E, Chang WT, Lim K, et al. Dysfunction in nonsense-mediated decay, protein homeostasis, mitochondrial function, and brain connectivity in ALS-FUS mice with cognitive deficits. Acta Neuropathol Commun 2021;9(1):9.
[23] Shiihashi G, Ito D, Arai I, Kobayashi Y, Hayashi K, Otsuka S, et al. Dendritic homeostasis disruption in a novel frontotemporal dementia mouse model expressing cytoplasmic fused in sarcoma. EBioMedicine 2017;24:102–15.
[24] Tibshirani M, Zhao B, Gentil BJ, Minotti S, Marques C, Keith J, et al. Dysregulation of chromatin remodelling complexes in amyotrophic lateral sclerosis. Hum Mol Genet 2017;26(21):4142–52.
[25] Frey D, Schneider C, Xu L, Borg J, Spooren W, Caroni P. Early and selective loss of neuromuscular synapse subtypes with low sprouting competence in motoneuron diseases. J Neurosci 2000;20(7):2534–42.
[26] Vinsant S, Mansfield C, Jimenez-Moreno R, Del Gaizo Moore V, Yoshikawa M, Hampton TG, et al. Characterization of early pathogenesis in the SOD1(G93A) mouse model of ALS: part II, results and discussion. Brain Behav 2013;3(4):431–57.
[27] Strey CW, Spellman D, Stieber A, Gonatas JO, Wang X, Lambris JD, et al. Dysregulation of stathmin, a microtubule-destabilizing protein, and up-regulation

of Hsp25, Hsp27, and the antioxidant peroxiredoxin 6 in a mouse model of familial amyotrophic lateral sclerosis. Am J Pathol 2004;165(5):1701–18.
[28] Kirola L, Mukherjee A, Mutsuddi M. Recent updates on the genetics of amyotrophic lateral sclerosis and frontotemporal dementia. Mol Neurobiol 2022;59(9):5673–94.
[29] Grassano M, Brodini G, De Marco G, Casale F, Fuda G, Salamone P, et al. Phenotype analysis of fused in sarcoma mutations in amyotrophic lateral sclerosis. Neurol Genet 2022;8(5):e200011.
[30] Picher-Martel V, Brunet F, Dupré N, Chrestian N. The occurrence of FUS mutations in pediatric amyotrophic lateral sclerosis: a case report and review of the literature. J Child Neurol 2020;35(8):556–62.
[31] Piol D, Robberechts T, Da Cruz S. Lost in local translation: TDP-43 and FUS in axonal/neuromuscular junction maintenance and dysregulation in amyotrophic lateral sclerosis. Neuron 2023;111(9):1355–80.
[32] Alecki C, Rizwan J, Le P, Jacob-Tomas S, Xu S, Minotti S, et al. Localized synthesis of molecular chaperones sustains neuronal proteostasis. bioRxiv 2023. https://doi.org/10.1101/2023.10.03.560761.
[33] Ahmed M, Spicer C, Harley J, Taylor JP, Hanna M, Patani R, et al. Amplifying the heat shock response ameliorates ALS and FTD pathology in mouse and human models. Mol Neurobiol 2023;60(12):6896–915.
[34] Wang WY, Pan L, Su SC, Quinn EJ, Sasaki M, Jimenez JC, et al. Interaction of FUS and HDAC1 regulates DNA damage response and repair in neurons. Nat Neurosci 2013;16(10):1383–91.
[35] Tejido C, Pakravan D, Bosch LVD. Potential therapeutic role of HDAC inhibitors in FUS-ALS. Front Mol Neurosci 2021;14:686995.
[36] Sullivan EK, Weirich CS, Guyon JR, Sif S, Kingston RE. Transcriptional activation domains of human heat shock factor 1 recruit human SWI/SNF. Mol Cell Biol 2001;21(17):5826–37.
[37] Atkinson BN, Woodward HL, Sipthorp J, Fish PV. Regioselective and enantiospecific synthesis of the HSP co-inducer arimoclomol from chiral glycidyl derivatives. Org Biomol Chem 2017;15(46):9794–9.
[38] Choi HJ, Cha SJ, Lee JW, Kim HJ, Kim K. Recent advances on the role of GSK3β in the pathogenesis of amyotrophic lateral sclerosis. Brain Sci 2020;10:675. https://doi.org/10.3390/brainsci10100675.
[39] Brown IR. Heat shock proteins and protection of the nervous system. Ann N Y Acad Sci 2007;1113:147–58.
[40] Chen S, Brown IR. Neuronal expression of constitutive heat shock proteins: implications for neurodegenerative diseases. Cell Stress Chaperones 2007;12(1):51–8.
[41] Chen S, Brown IR. Translocation of constitutively expressed heat shock protein Hsc70 to synapse-enriched areas of the cerebral cortex after hyperthermic stress. J Neurosci Res 2007;85(2):402–9.
[42] Nakano I, Hirano A. Atrophic cell processes of large motor neurons in the anterior horn in amyotrophic lateral sclerosis: observation with silver impregnation method. J Neuropathol Exp Neurol 1987;46:40–9.
[43] Carpenter S, Karpati G, Durham H. Dendritic attrition precedes motor neuron death in amyotrophic lateral sclerosis (ALS). Neurology 1988;34:252.
[44] Calvo A, Moglia C, Canosa A, Manera U, Vasta R, Grassano M, et al. High frequency of cognitive and behavioral impairment in amyotrophic lateral sclerosis patients with SOD1 pathogenic variants. Ann Neurol 2024;96:150–8.